Evaluation of Abdominal Injury Risk Prediction from Seatbelt Loading

Devon L. Albert, Allison J. Guettler, Andrew R. Kemper, Warren N. Hardy

Abstract This study pooled the data from nine previous studies to develop and evaluate new injury risk curves to predict AIS2+ and AIS3+ abdominal injuries from belt loading. The evaluated predictors were based on lap belt force, abdominal compression (Cmax), rate of compression (Vmax), and pressure in the abdominal vasculature. Injury risk curves were generated using logistic regression and survival analysis via non-parametric methods and parametric methods with three distributions. The fit and predictive ability of each injury risk curve were assessed using multiple methods. The purely rate-based metrics, Vmax and P' (rate of pressure) were not significant predictors for either injury threshold. All other predictors were significant for at least one injury risk curve among the different distributions and injury thresholds tested. The best predictors for AIS2+ injuries were pressure and lap belt force. The best predictor for AIS3+ injuries was V*C. Pressure was a good predictor for both injury risk thresholds. This indicates that abdominal vascular pressure is a promising metric for abdominal injury risk predictions.

Keywords Abdominal compression, belt force, pressure, rate of compression, rate of pressure

I. INTRODUCTION

The use of a seatbelt reduces the risk of injuries in frontal motor vehicle collisions, but the seatbelt is still a common source of abdominal organ injuries [1]. Furthermore, abdominal injury from seatbelt loading may increase as automation in vehicles increases. Reclined occupants are already associated with higher mortality and injury risk [2], with belted occupants being more likely to sustain abdominal injuries when reclined due to the increased propensity for submarining [3-4]. As more occupants are anticipated to recline their seats as automation becomes more prevalent and advanced, submarining and abdominal injuries are expected to increase. Furthermore, with more flexibility in seating configurations, seats might move occupants farther away from forward structures, such as the instrument panel and knee bolster. Removing the loading path between these structures and the lower extremities of the occupants will place more burden on the lap belt to restrain occupants. This may increase loads transmitted from the lap belt to the occupant and increase abdominal injury risk, as well.

Currently, there is no consensus on the most effective metric to predict abdominal injury risk due to belt loading. Belt force, abdominal compression, rate of abdominal compression, and combinations thereof have all been assessed as potential predictors [5-14]. However, the best predictor typically varies between studies as each study uses different datasets, different methods to generate injury risk curves, and different evaluation criteria. Metrics derived from pressure measured in the abdominal vasculature have also been correlated with abdominal injury, particularly liver injuries [9][15-16]. Abdominal pressure sensors have been introduced into anthropomorphic test devices (ATDs) to assess submarining and injury risk [17-21]. Injury risk curves for the Q-series child ATDs were developed by reconstructing injurious motor vehicle collision scenarios in the laboratory, linking the ATD response to the real-world injuries [20-21]. With the ability to instrument post-mortem human subjects (PMHS) with sensors to measure pressure in the abdomen during biomechanical tests [5,9,22,23], PMHS damage can be directly linked to pressure thresholds. Subsequently, human injury risk curves can be established and mapped to ATD sensors to more accurately predict injury for other demographics.

PMHS biomechanical and damage data have been used to generate injury risk curves based on belt force, abdominal compression, rate of compression, and pressure [6][9][11][14-15]. Pressure-based injury risk curves in

D. L. Albert (e-mail: dla16@vt.edu; tel: +1-540-231-1890) is a Research Assistant Professor, A. J. Guettler is a Postdoctoral Associate, A. R. Kemper is an Associate Professor, and W. N. Hardy is an Associate Professor and Director in the Center for Injury Biomechanics (CIB) at Virginia Tech in Blacksburg, VA, USA.

particular have been constructed using limited data from only one to three studies [9][15]. However, biomechanical data, including pressure measurements, are now available from more studies and can be used to assess potential abdominal injury risk predictors more comprehensively. Therefore, the purpose of this study was to pool data from previous studies to develop and evaluate updated injury risk curves for predicting abdominal injuries due to seat belt loading.

II. METHODS

Literature Search

A literature search was performed to find all available and applicable data that could be used to develop risk curves to predict abdominal injury from seatbelt loading. Several inclusion criteria were applied to determine if a study would be included in the dataset. First, loading needed to be primarily in the frontal direction and from the seatbelt. The presence of other loading mechanisms led to exclusion. Second, studies had to involve unembalmed PMHS. Third, the studies needed to report lap belt load and either abdominal displacement/compression or vascular pressure within the abdomen. Last, a post-test dissection of the abdomen was required, and abdominal damage, when present, needed to be reported. For all studies, only abdominal organ, mesentery, and vascular damage was considered. Skeletal damage, i.e. to the lumbar spine and pelvis, was excluded. The diaphragm was considered part of the thorax, in accordance with the 2015 version of the Abbreviated Injury Scale (AIS) [24].

Ten studies met the above inclusion criteria. However, the PMHS in one study underwent additional tests that loaded the pelvis or thorax between the abdominal loading tests and dissection [8]. Previous studies have discussed uncertainty regarding when the abdominal damage observed during these tests occurred due to two factors [7][11]. First, the subsequent tests had the potential to induce abdominal damage, since the pelvis and thorax, which are in close proximity to the abdomen, were targeted. Second, the time needed to conduct multiple impacts in multiple configurations may have led to increased soft tissue degradation in the abdomen, making it more likely to sustain damage during the latter tests. Due to the uncertainty regarding when the abdominal injuries were sustained, the study was excluded from this analysis [11]. The nine remaining studies were included in this analysis. Brief descriptions of each test are included below.

Hardy *et al.* performed two abdominal belt pull tests each on three upright PMHS for a total of six tests [6]. Belt force and abdominal displacement were measured. No abdominal damage was observed so the maximum value measured for each parameter between the two tests performed on each PMHS was treated as right censored.

Steffan *et al.* conducted tests where the seatbelt was cinched around the abdomen of 14 PMHS seated in a rigid seat with an adjustable seatback [12]. Belt force and abdominal displacement were measured, but rate of penetration was not reported. Both damage and non-damage outcomes were observed.

Trosseille *et al.* conducted tests on six upright PMHS where the belt was pulled into the abdomen via pretensioners [13]. Belt force and abdominal displacement were measured. Both damage and non-damage cases were observed. One PMHS had existing abdominal damage prior to testing and was excluded from this analysis.

Foster *et al.* conducted tests on nine upright PMHS where the belt was pulled into the abdomen via pretensioners [5]. Belt force, abdominal displacement, and abdominal vascular pressure were measured. Both damage and non-damage cases were observed.

Untaroiu *et al.* conducted four static pretensioner tests where PMHS were seated in a production seat wearing a three-point seat belt [14]. Lap belt force and abdominal displacement were measured. Both damage and non-damage cases were observed.

Howes *et al.* conducted tests on six PMHS in either an upright (n=2) or inverted (n=4) position under three-point belt loading [7]. Lap belt force, abdominal displacement, and pressure inside the jejunum were measured. Since pressure measured inside a hollow organ may not be comparable to pressure measured inside the vasculature, the jejunum pressures were not included in this analysis. All PMHS sustained AIS2+ damage.

Ramachandra *et al.* conducted two separate belt-pull test series on two populations of PMHS. The first test series was conducted on seven PMHS [9][10]. Four of the PMHS were tested once and three PMHS were tested twice, where the first test was designed to be non-damaging. Both damage and non-damage cases were observed. If any damage was observed for the PMHS tested twice, it was assumed the damage occurred during the second test, as suggested by the authors. The second test series was conducted on six PMHS with 5th percentile female anthropometry. Three of the tests were designed to be non-damaging, while three were designed to be damaging. Therefore, both damage and non-damage cases were observed. Both test series measured belt force, abdominal displacement, and abdominal vascular pressure.

Guettler et al. conducted 12 sled tests (ΔV=56 km/h) with 50th percentile male PMHS seated in the second row of four different vehicle bucks [22]. PMHS were either restrained with a standard three-point belt or a three-point belt with a pretensioner and load limiter. Lap belt force and abdominal vascular pressure were measured. Both damage and non-damage cases were observed with regard to the abdomen.

The following parameters were collected from each study, as available: peak lap belt force (PBF), maximum depth of belt penetration into the abdomen (Dmax), maximum percent compression of the abdomen normalised by abdomen depth (Cmax), maximum rate of lap belt penetration into the abdomen (Vmax), the abdominal injury criterion, i.e., the product of Vmax and Cmax (Vmax*Cmax), the maximum of the time aligned product of rate of penetration and percent compression (V*C), the product of PBF and Cmax (Fmax*Cmax), peak vascular pressure in the abdomen (P), peak rate of pressure (P'), and the product of P and P' (P*P'). Preliminary analyses indicated much larger variance in Dmax compared to Cmax, so Dmax was excluded in favor of Cmax. The compiled parameter data and injury outcomes for all studies are included in Tables AI, AII, and AXII in the Appendix.

Predictor Evaluation

Two datapoints were excluded from the pressure data. One test from [22] and one test from [10] resulted in unusually high peak pressure and rate of pressure. In both cases, it was unclear whether the recorded pressures were accurate or caused by direct contact with a solid structure. Therefore, the pressures and their derivatives for both tests were excluded from the analysis.

Similar to the methodology used by previous studies, the linear correlation between predictors was evaluated prior to risk curve generation to determine whether it would be possible to perform any multivariate analyses [11][14]. The Pearson Correlation Coefficient was calculated for each possible pair of predictors, and the significance of the correlation was assessed using a Student's t-test. Each predictor was significantly correlated with multiple other predictors (Table AII), which indicated the predictors were not necessarily independent of each other. Therefore, it was not appropriate to combine them into multivariate analyses, so risk curves were limited to univariate analyses.

Risk Curve Generation and Evaluation

Univariate injury risk curves were fitted to each parameter using both AIS2+ and AIS3+ as the injury outcome threshold. Data were considered left or right censored, depending on whether the sustained damage met the applied injury threshold, i.e. AIS2+ or AIS3+. Two injury risk curve methods were used. First, logistic regression models were fit to each predictor. The significance of the predictor was tested using the Wald chi-square test statistic (χ^2). A p-value less than 0.05 indicated that the predictor made a significant contribution to the model. Second, survival analysis was used to generate risk curves via non-parametric and parametric methods. The non-parametric curves were computed using Turnbull estimates and were used to evaluate how well the parametric curves fit the distribution of the underlying data. The parametric distributions included Weibull, lognormal, and loglogistic. All injury risk curves were generated using JMP Pro 16 (JMP Statistical Discovery LLC, Cary, NC, USA). The 95% confidence intervals were calculated for all parametric survival curves. The relative size of the confidence intervals (RSCI) were evaluated at 5%, 25%, and 50% probability by dividing the width of the confidence intervals by the value of the predictor at these locations [25]. Smaller values of RSCI indicate narrower confidence intervals, and higher confidence in the prediction at that injury probability.

The predictive performance of the logistic and parametric survival curves was evaluated for each predictor and injury threshold. The corrected Akaike Information Criterion (AICc) was calculated to compare predictive performance between distributions, where a lower value indicated better predictive performance. Then, Goodman and Kruskal's gamma (γ) was computed for each injury risk curve relative to the true damage data, assuming an injury threshold of 50% risk of injury. A t-distribution was used to test the significance of γ, i.e. whether the predictions of each curve were significantly correlated with actual injury outcomes. Goodman and Kruskal's gamma was chosen to allow direct comparisons to a previous study [9]. Furthermore, this method allows the probability predicted by the injury risk curve to be converted to a binary outcome, which can then be directly compared to the true binary injury outcome. Injury assessment reference values are often established from a threshold on an injury risk curve and used in the same manner. The drawback of this approach is that it does not account for the proximity of the predicted injury risk to the assumed injury threshold. To compensate for this limitation, the point-biserial correlation coefficient (r_{pb}) was also calculated to evaluate whether the predicted injury probabilities and actual injury outcomes were linearly correlated. The significance of the correlation was

evaluated using the t-distribution. Both γ and r_{pb}, range from -1 to 1, where -1 indicates a strong negative correlation, 1 indicates a strong positive correlation, and 0 indicates no correlation. This analysis was performed using the same data used to generate the injury risk curve as no test dataset was available for all predictors.

III. RESULTS

Eighteen non-parametric risk curves were generated, and 69 parametric risk curves were generated (Tables AIII–AIV, Fig. 1–9). Three injury risk curves did not converge to a solution, namely the three parametric survival curves for Vmax. AICc values were generally similar within a predictor, indicating there was little difference in performance between different parametric models (Table I). The model with the lowest AICc value varied with predictor and injury risk threshold.

The non-parametric injury risk curves for many predictors displayed large steps (Fig. 3, 4, 9). Large steps reduce the ability to use the non-parametric curves to assess the fit of the parametric curves, and indicate that the dataset for the predictor is less able to inform injury risk prediction in that area. This could be a result of the data having poor predictive ability or the presence of multiple injury mechanisms. The non-parametric survival curves for Fmax*Cmax exhibited undefined regions toward the ends of the curves because the largest non-injury value exceeded the largest injury value.

In accordance with their similar AICc values, the parametric curves were generally similar within a predictor and injury threshold. Although, the logistic injury risk curves tended to diverge from the rest of the risk curves toward beginning and ends of the curves (Fig. 3, 8). The logistic curves also predicted non-trivial injury risk at zero stimulus for several predictors, making them inaccurate representations of injury risk (Fig. 3,6,8,9).

TABLE I
AICc VALUES FOR AIS2+ AND AIS3+ INJURY PREDICTION

	AIS2+				AIS3+			
	Lognormal	Weibull	Loglogistic	Logistic	Lognormal	Weibull	Loglogistic	Logistic
PBF	77.81	78.37	77.90	79.43	76.30	76.42	76.35	76.90
Cmax	72.10	72.00	72.06	71.93	53.27	53.90	53.53	54.40
Vmax	59.23	59.14	59.23	58.31	-	-	-	51.34
*Vmax*Cmax*	51.83	52.10	52.00	52.65	45.61	45.67	45.77	46.07
*V*C*	56.76	56.35	56.79	55.61	42.51	42.26	42.58	42.39
*Fmax*Cmax*	65.33	66.48	65.36	69.25	52.53	53.60	52.89	55.84
P	35.97	35.53	36.12	35.65	39.15	38.08	39.08	37.62
P'	44.70	44.68	44.71	44.55	45.97	46.00	45.99	46.10
*P*P'*	40.80	41.06	40.83	42.25	42.60	42.86	42.69	44.12

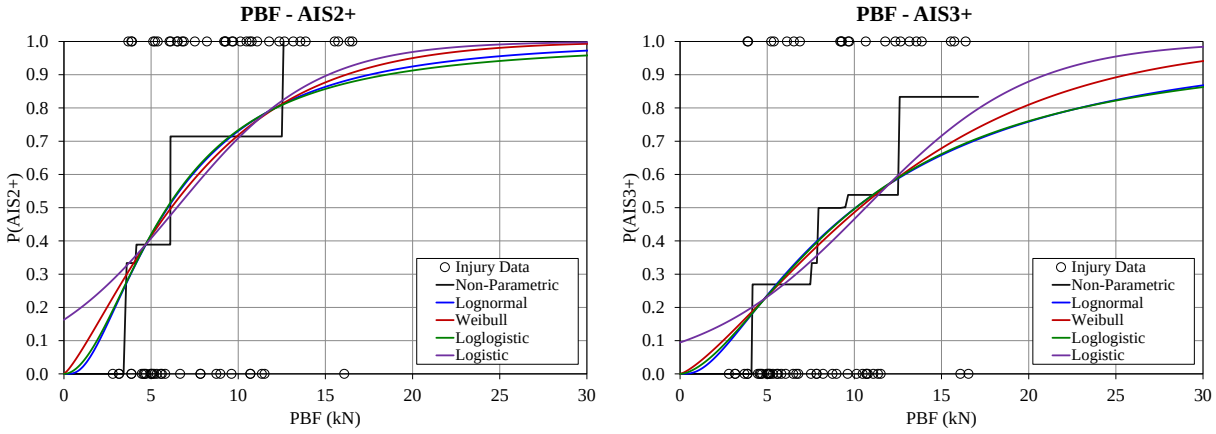

Fig. 1. AIS2+ (left) and AIS3+ (right) injury risk functions using Peak Belt Force.

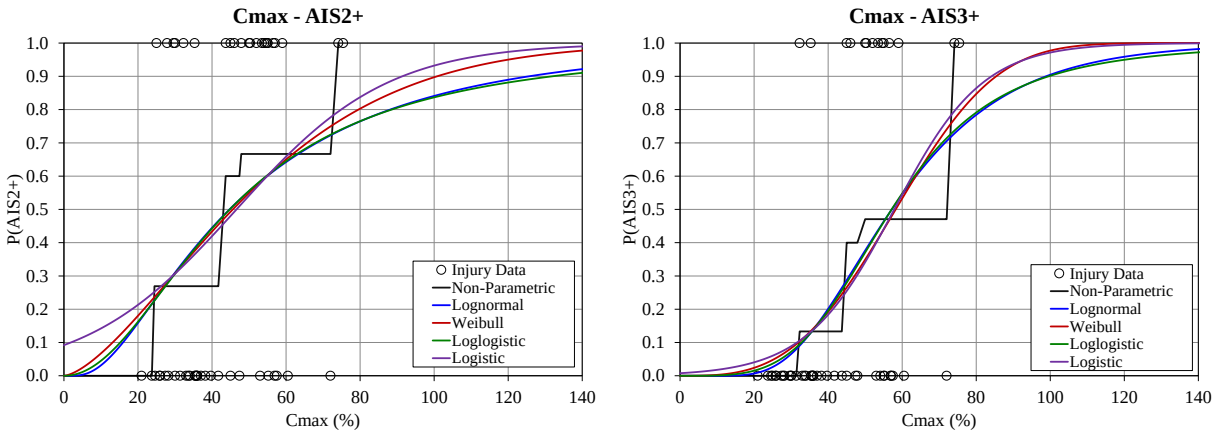

Fig. 2. AIS2+ (left) and AIS3+ (right) injury risk functions using Cmax.

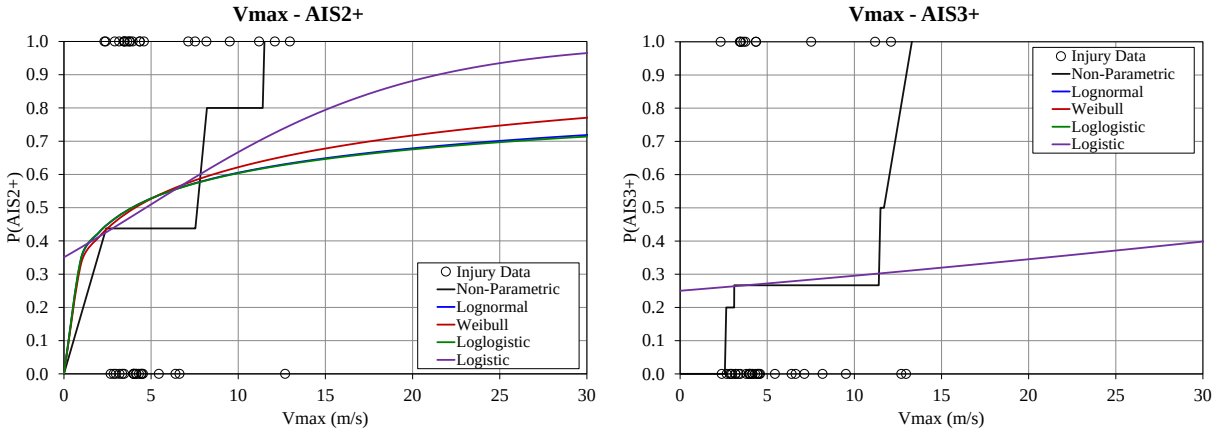

Fig. 3. AIS2+ (left) and AIS3+ (right) injury risk functions using Vmax.

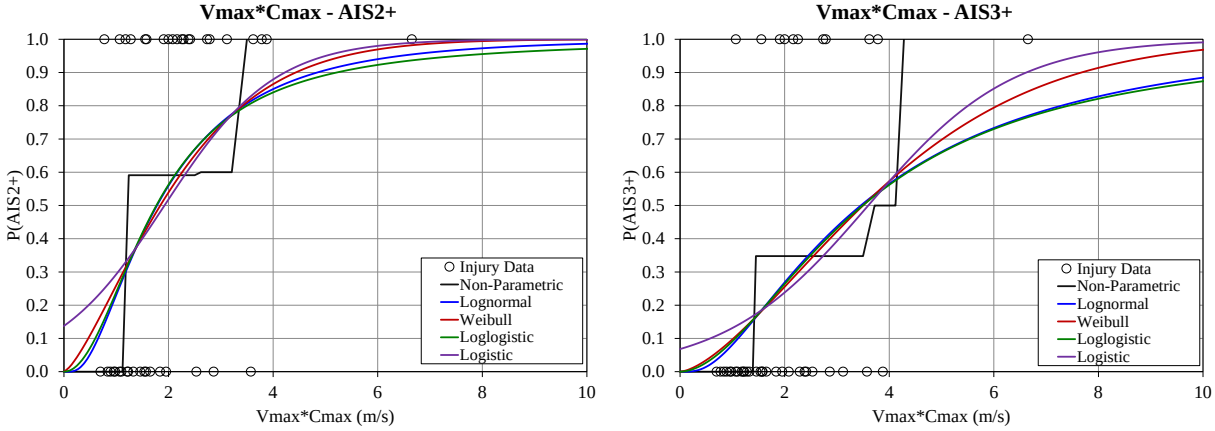

Fig. 4. AIS2+ (left) and AIS3+ (right) injury risk functions using Vmax*Cmax.

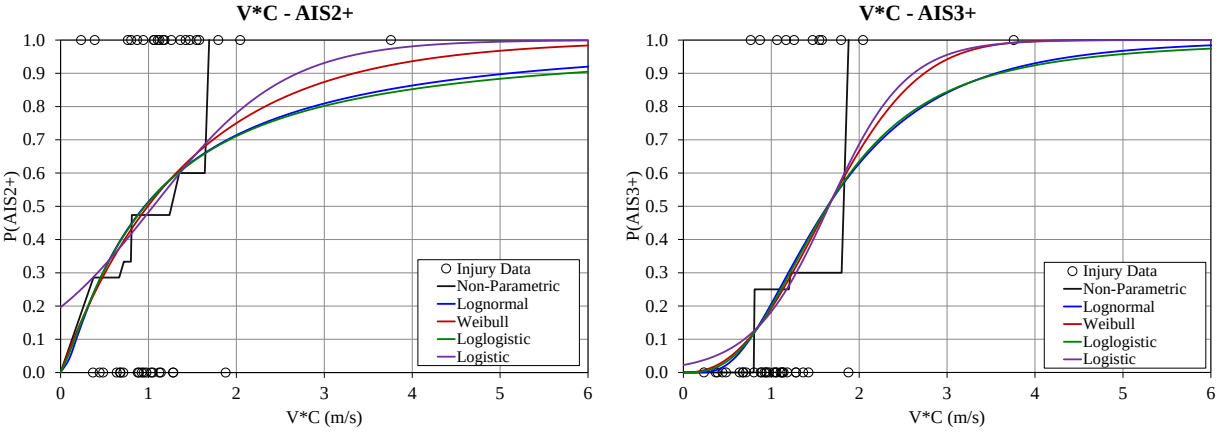

Fig. 5. AIS2+ (left) and AIS3+ (right) injury risk functions using V*C.

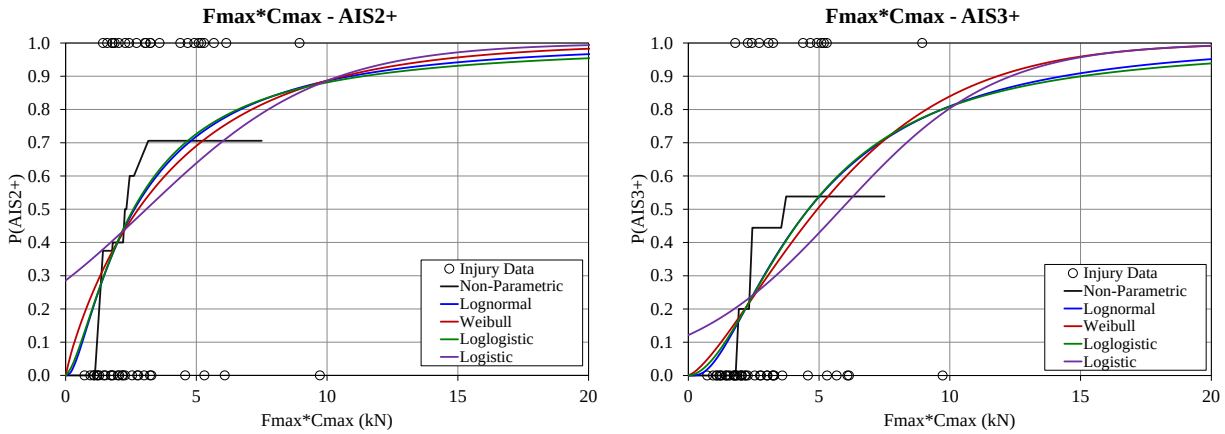

Fig. 6. AIS2+ (left) and AIS3+ (right) injury risk functions using Fmax*Cmax.

The χ^2 statistic was used to determine whether a predictor significantly contributed to the logistic regression model. PBF, Cmax, and P were all significant at both injury thresholds. Vmax*Cmax was only significant for the AIS2+ model, whereas V*C and Fmax*Cmax were only significant for the AIS3+ model.

The γ and r_{pb} statistics were used to assess how well the injury risk curve predictions correlated to actual injury outcomes. The correlation statistics for each curve are shown in Tables II-V, while the associated p-values are shown in Tables AVI-AIX in the Appendix. The curves with significant predictive ability varied depending on the test statistic, distribution, and injury threshold. For γ, P and P*P' had the highest correlation with the AIS2+ injury outcome and were statistically significant across most distributions (Table II). PBF, Cmax, and Fmax*Cmax were also statistically significant for most distributions. For the AIS3+ injury outcome, V*C and P had the highest correlations (Table III). V*C and P were significant across all distributions, while PBF was only significant for the lognormal and loglogistic curves.

More predictors were statistically significant using r_{pb} for both injury thresholds compared to γ. PBF, Cmax, Vmax*Cmax, Fmax*Cmax, and P were all significant predictors for all distributions at both injury thresholds (Tables IV-V). For the AIS3+ outcome, V*C was significant for all distributions, while P*P' was only significant for some distributions. Across both injury thresholds, P had the highest correlations.

Analysing these results collectively, only Vmax and P' did not have any significant predictability across all combinations of distribution, test statistic, and injury threshold. Both Vmax and P' were the only predictors that were purely rate-based. Other predictors that combined Vmax and P' with other non-rate parameters, i.e. Vmax*Cmax, V*C, and P*P', had significant predictive ability in some situations. On the other hand, P appeared to be the most consistently good predictor across test statistics, injury thresholds, and distributions.

TABLE II
GOODMAN KRUSKAL GAMMA AND CHI SQUARED (LOGISTIC) VALUES FOR AIS2+ INJURIES
STATISTICS WITH P-VALUES LESS THAN 0.05 ARE BOLDED

	Lognormal	Weibull	Loglogistic	Logistic	Logistic
	γ	γ	γ	γ	χ^2
PBF	**0.71**	**0.71**	**0.71**	**0.68**	**8.02**
Cmax	**0.68**	**0.68**	**0.68**	**0.63**	**4.75**
Vmax	-0.13	-0.02	-0.13	0.22	1.28
*Vmax*Cmax*	0.55	0.47	0.55	0.39	**4.84**
*V*C*	0.08	0.08	0.08	0.19	2.89
*Fmax*Cmax*	**0.66**	**0.66**	0.58	**0.66**	3.51
P	**0.76**	**0.76**	**0.76**	0.68	**6.84**
P'	0.48	0.48	0.48	-	0.97
*P*P'*	**0.76**	**0.76**	**0.76**	**0.76**	2.11

TABLE III
GOODMAN KRUSKAL GAMMA AND CHI SQUARED (LOGISTIC) VALUES FOR AIS3+ INJURIES
STATISTICS WITH P-VALUES LESS THAN 0.05 ARE BOLDED

	Lognormal γ	Weibull γ	Loglogistic γ	Logistic γ	Logistic χ^2
PBF	**0.65**	0.59	**0.65**	0.45	**6.95**
Cmax	0.53	0.67	0.53	0.67	**8.38**
Vmax	-	-	-	-	0.04
*Vmax*Cmax*	0.67	0.67	0.67	0.83	3.84
*V*C*	**0.77**	**0.77**	**0.77**	**0.77**	**5.44**
*Fmax*Cmax*	0.35	-0.03	0.35	0.19	**5.08**
P	**0.74**	**0.80**	**0.74**	**0.72**	**6.49**
P'	0.05	0.05	0.05	-0.11	1.05
*P*P'*	0.64	0.43	0.64	0.05	1.74

TABLE IV
POINT-BISERIAL CORRELATION COEFFICIENTS FOR AIS2+
COEFFICIENTS WITH P-VALUES LESS THAN 0.05 ARE BOLDED

	Lognormal	Weibull	Loglogistic	Logistic
PBF	**0.415**	**0.407**	**0.414**	**0.388**
Cmax	**0.312**	**0.315**	**0.313**	**0.317**
Vmax	0.103	0.113	0.103	0.177
*Vmax*Cmax*	**0.407**	**0.400**	**0.405**	**0.386**
*V*C*	0.260	0.272	0.259	0.294
*Fmax*Cmax*	**0.382**	**0.362**	**0.383**	**0.289**
P	**0.525**	**0.529**	**0.524**	**0.527**
P'	0.183	0.183	0.182	0.181
*P*P'*	**0.388**	**0.377**	**0.389**	0.315

TABLE V
POINT-BISERIAL CORRELATION COEFFICIENTS FOR AIS2+
COEFFICIENTS WITH P-VALUES LESS THAN 0.05 ARE BOLDED

	Lognormal	Weibull	Loglogistic	Logistic
PBF	**0.359**	**0.360**	**0.360**	**0.356**
Cmax	**0.446**	**0.437**	**0.443**	**0.429**
Vmax	-	-	-	0.034
*Vmax*Cmax*	**0.357**	**0.360**	**0.356**	**0.356**
*V*C*	**0.455**	**0.465**	**0.457**	**0.468**
*Fmax*Cmax*	**0.381**	**0.363**	**0.377**	**0.319**
P	**0.493**	**0.519**	**0.497**	**0.531**
P'	0.204	0.201	0.203	0.187
*P*P'*	**0.364**	0.353	**0.362**	0.294

Qualitatively, issues with the Vmax and P' parametric injury risk curves were observed that might contribute to their lack of predictive ability. For Vmax, the parametric curves did not fit the underlying data distribution, as indicated by the shape of the non-parametric risk curves (Fig. 3). The logistic curve for Vmax for AIS3+ injuries was essentially flat over the range where the injury and non-injury data points occurred. Additionally, these predictors were all cases where the logistic risk curves predicted a nontrivial risk of AIS2+ and AIS3+ injuries at zero stimulus. For P', the logistic injury risk curves indicated at least a 40% and 30% risk of AIS2+ and AIS3+ injury, respectively, at zero stimulus value (Fig. 9). The survival parametric curves were initially very steep, allowing the curves to reach the 50% risk of injury threshold quickly and at low values of P'.

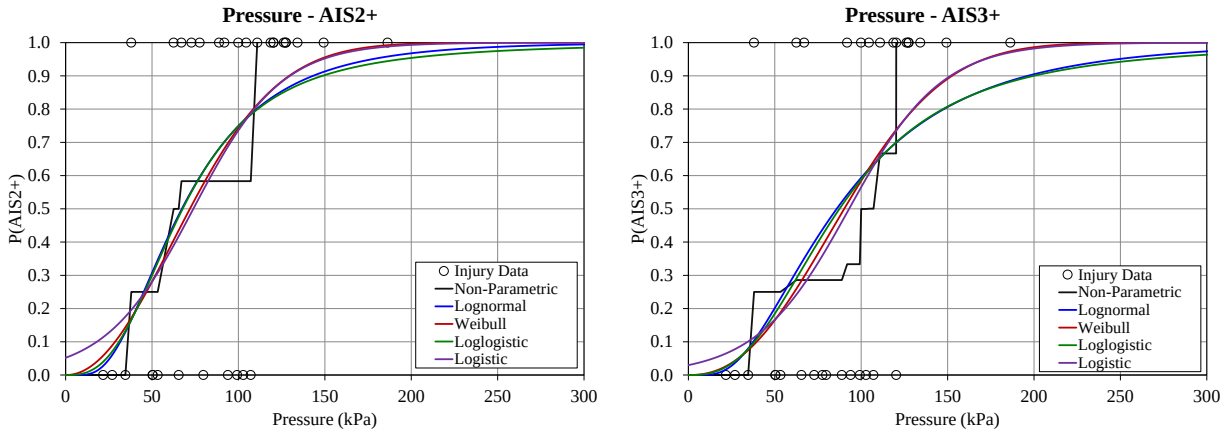

Fig. 7. AIS2+ (left) and AIS3+ (right) injury risk functions using Pressure.

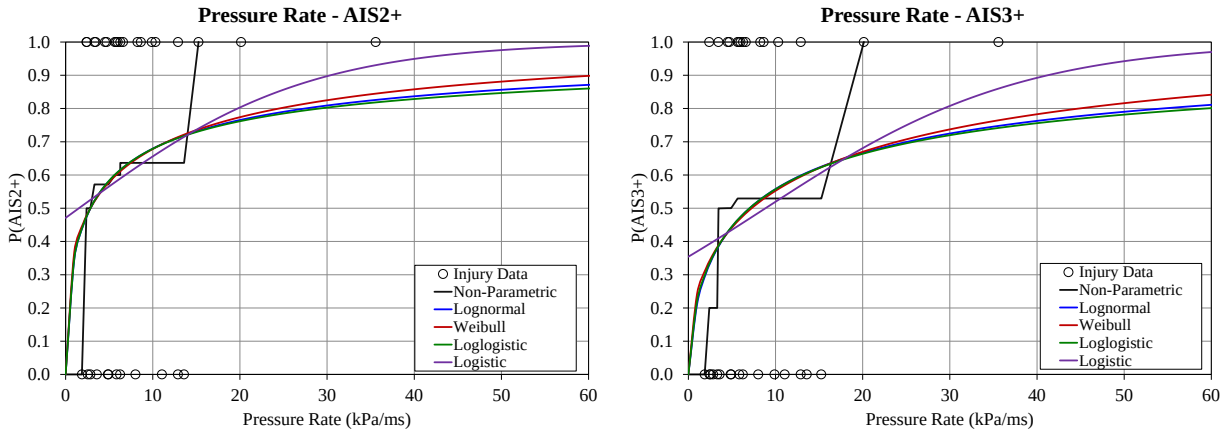

Fig. 8. AIS2+ (left) and AIS3+ (right) injury risk functions using Pressure Rate.

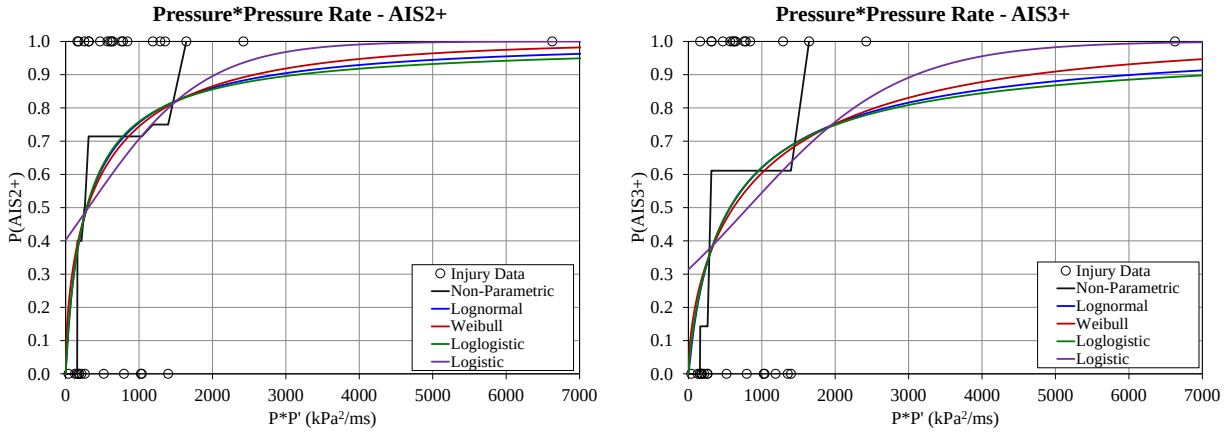

Fig. 9. AIS2+ (left) and AIS3+ (right) injury risk functions using Pressure*Pressure Rate.

Due to the issues noted above with the logistic regression curves, 95% confidence intervals were only calculated for the parametric survival analysis curves. Confidence intervals tended to be similar widths across distributions, so exemplar confidence intervals were plotted for the lognormal distribution (Fig. A1-A9). The RSCI for all distributions were evaluated on a qualitative scale where less than 0.5 corresponded to good, between 0.5 and 1 corresponded to fair, and between 1 and 1.5 corresponded to marginal, and greater than 1.5 was unacceptable [25]. The width of the confidence intervals differed between the AIS2+ and AIS3+ thresholds. For AIS2+, P had the lowest RSCI values on average, followed by PBF (Table AX). Both predictors fell within the marginal range, on average. The remaining predictors were classified as unacceptable based on average RSCI: Vmax, Vmax*Cmax, V*C, P', and P*P'. For AIS3+, Cmax and V*C had the lowest RSCI values, and were classified as fair (Table AXI). PBF, Vmax*Cmax, Fmax*Cmax, and P were classified as marginal. P' and P*P' were unacceptable. RSCI could not

be computed for Vmax at the AIS3+ threshold because the parametric curves did not converge.

IV. DISCUSSION

Sixty-nine parametric injury risk curves were generated in this study. The predictive ability of the curves varied with predictor, distribution, and injury threshold. For AIS2+ injuries, PBF, Cmax, and P were consistently good predictors across all metrics. However, only P and PBF had RSCI values within the acceptable range. For AIS3+ injuries, P and V*C were consistently good predictors. Cmax and V*C had the best confidence intervals for AIS3+, while P was in the acceptable range. Vmax and P' were the poorest predictors across all metrics. These results were compared to the results of previous studies that evaluated abdominal injury predictors using smaller datasets.

Rouhana *et al.* analysed a subset of the current dataset, including [5-6][12-13], using logistic regression [11]. Goodness of fit and predictive ability were evaluated using the Pearson Goodness of Fit and Goodman and Kruskal's Gamma. They reported that Vmax*Cmax was the best predictor for both AIS2+ and AIS3+ injuries. It should be noted that Vmax performed well as a predictor, but not as well as Vmax*Cmax. These results partially align with the results of the current study in that Vmax*Cmax was a fair predictor for AIS3+ injuries, while V*C, closely related to Vmax*Cmax, was a good predictor of AIS3+ injuries. The results regarding Vmax do not align between the studies as the current study found that Vmax was a poor predictor.

Untaroiu *et al.* analysed the same dataset as [11], but added four additional datapoints [14]. Again, logistic regression was used to generate injury risk curves for AIS2+ and AIS3+ injuries. Vmax and Fmax*Cmax were reported as the best predictors for AIS2+ and AIS3+ injuries, respectively. These results do not align as well with the results of the current study, where Vmax was a poor predictor. In the current study, the predictive ability of Fmax*Cmax varied with distribution and injury threshold, and better, more consistent predictors were observed.

Ramachandra *et al.* combined the data from their study with two previous studies on liver injury risk [15-16] to generate novel pressure-based injury risk curves for AIS3+ injuries [9]. They reported that the injury risk curve with the best predictive ability used P' and leveraged the data from all three studies. They also combined their Vmax, Vmax*Cmax, and Fmax*Cmax values with those from [11] to generate additional injury risk curves. They reported that Vmax*Cmax was the best predictor of AIS3+ injuries of the three predictors evaluated. It should be noted that all injury risk curves in this study assumed a Weibull distribution. While Ramachandra et al. observed that P' was a good predictor, the opposite was true in this study. The reasons behind this discrepancy will be explored in the next section.

Throughout the previous studies and the current study, compression-based predictors, i.e., Vmax*Cmax, V*C, and Fmax*Cmax, showed fair to good predictive ability. However, previous studies reported that Vmax was a good predictor, while the current study observed that it was the poorest predictor. The Vmax dataset used in the current study was essentially two times the size of the datasets used by Untaroiu *et al.* and Rouhana *et al.* Furthermore, the values of Vmax reported in the more recent studies [7][9-10] encompassed in the current study tended to be smaller than those encompassed by the previous studies [5-6][12][14]. Therefore, inherent differences may exist between the datasets that influence the disparate results for Vmax.

Pressure and Rate of Pressure: Comparisons to Literature

Due to the novelty of pressure-based abdominal injury risk prediction relative to the other predictors evaluated, the differences between the results of the current study and the Ramachandra *et al.* study were explored in more detail. As mentioned above, Ramachandra *et al.* observed that P' was a good predictor of AIS3+ injury risk, while the current study found that P' was a poor predictor for both AIS2+ and AIS3+ injuries [9]. Additionally, P was a good predictor at both injury thresholds in the current study. Ramachandra *et al.* did not directly assess P as a predictor, only P' and P*P'. Therefore, a pressure-based Weibull injury risk curve was generated using the same data as Ramachandra *et al.* so that all three predictors could be compared between both studies at the AIS3+ injury threshold.

Injury risk curves from the current study and the Ramachandra study are compared in Fig. A10 and Fig. A11. The curve for pressure is shifted to the right for the current study relative to the Ramachandra curve. This indicates that a higher pressure is needed to generate injury given the data in the current study compared to the data used by [9]. The risk curves for P' are quite different between the two studies. The curve for the current study is steeper initially, but becomes flatter and very slowly approaches 100% risk of injury. Conversely, the

Ramachandra curve is steeper in the middle of the curve and approaches 100% risk of injury quickly. Surprisingly, the two curves yield a similar threshold for 50% risk of injury, despite their differences. The P*P' risk curves are similar for both studies until the 50% risk threshold is reached. Then the curves diverge, with the Ramachandra curve retaining a steep slope and reaching 100% risk of injury more quickly.

Goodman and Kruskal's gamma was used in both studies to assess the predictive ability of the curves using the same dataset that was used to generate the curves. To quantitatively assess whether the results observed in each study were specific to the test data evaluated, the Goodman and Kruskal's gamma was recalculated for the curves from the current study using the test data from [9][15-16], which was the same dataset used to generate the Ramachandra risk curves. The results indicated that P was not a significant predictor (γ=0.500, p=0.450), P' was significant predictor (γ=0.872, p=0.0008), and P*P' was a significant predictor (γ=0.864, p=0.0028). These results are the opposite of those observed when Goodman and Kruskal's gamma is calculated using the data from the current study. Therefore, it is apparent that Goodman and Kruskal's gamma relies heavily upon what test data are used to evaluate the curve. The data from [9][15-16], appear to be more correlated with P' than the data in the current study. This observation is reinforced by calculating the area under the receiver operating characteristic curve (AUC) for dataset from the current study, the Ramachandra study, and both combined. AUC is independent of the method of generating the injury risk curve and only depends upon the test dataset used to generate the statistic. Hence, the values reveal which predictor is the best for a given dataset, regardless of the injury risk curve applied. For the dataset from the current study, P has the best AUC and P' has the worst (Table IV). For the Ramachandra *et al.* dataset, all three predictors have similar values, but P' has the highest. When the two datasets are combined, the values become less disparate compared to the results from the current study, but P still has the highest AUC and P' the smallest.

As discussed above, Ramachandra *et al.* combined the pressure data from their study with two other studies on liver injury to build a large enough sample size to generate injury risk curves. One of these studies tested *ex vivo* livers and measured the pressure inside the vasculature [16]. The other study tested whole PMHS under oblique and lateral loading to the abdomen [15]. Both studies involved blunt impactor loading, as opposed to belt loading, which is why they did not meet the inclusion criteria for the current study. They also only assessed liver damage, while the studies included in the current study assessed abdominal damage as a whole.

These differences may explain why the Ramachandra *et al.* results were so different from those of the current study. The majority of damage in that dataset was to the liver, while the current dataset includes damage to solid organs, hollow organs, mesentery, and abdominal vasculature. All of these structures may have different injury mechanisms, which may have varying sensitivity to rate. Injury to the solid organs, such as the liver, may be more rate dependent. This would explain why the Ramachandra *et al*. dataset, which is largely composed of liver damage, indicates that P' is a good predictor while the current study does not. It may be necessary to consider P*P' as a more universal predictor for abdominal injury, even though it was not a significant predictor for AIS3+ injuries in the current study, because it is able to capture injury mechanisms that are and are not dependent on rate effects.

TABLE IV
AUC VALUES FOR DIFFERENT TEST DATASETS

	Current Study	Ramachandra *et al.* 2016	Combined
P	0.796	0.779	0.751
P'	0.542	0.785	0.649
*P*P'*	0.633	0.779	0.721

Limitations

Several limitations to the study must be discussed. As noted above, the Goodman and Kruskal's gamma analysis is highly sensitive to the test data used in its calculation. For both the current study and previous studies, the same data used to generate the injury risk curves were also used to evaluate the curves. This can bias the conclusions drawn from the analysis, but it also maximises the amount of data that can be used to train and test the injury risk curves.

It should be noted that different sample sizes were available to generate the injury risk curves for each

predictor, depending on what predictors were reported by previous studies and whether there were any excluded or missing data. PBF had the largest sample size in this analysis, which would give it the most statistical power. It was one of the best predictors for AIS2+ injuries, but not AIS3+ injuries.

This study combined data from several different studies with a variety of test setups, PMHS positions, and other methodologies. Combining all of this data together could have increased the variance in the predictor data and weakened the resulting injury risk curves. However, encompassing many different test setups allows the curves to be applied more widely across different scenarios. Similarly, this study focused on abdominal injury risk as a whole, meaning the data could encompass different injury mechanisms for different organs, i.e., hollow or solid organs. Damage to the hollow and solid organs were observed at similar frequencies in the dataset (Table AXII). They were also often observed during the same test, which made it difficult to isolate injury mechanisms that may be specific to different types of organs. Despite the similar prevalence of different organ injuries in this dataset, predictors may still be more or less accurate for different injuries. Furthermore, the distribution of injuries across organ types may also be a contributing factor to the varying results observed across studies evaluating abdominal injury risk criteria.

Muscle tension plays an important role in the response of the abdomen during biomechanical tests. The loss of muscle tension post-mortem combined with the effect of gravity causes the abdominal contents to displace further downward in PMHS compared to human subjects. This can affect the biomechanical response of the abdomen to loading, as different structures may be loaded in a test using PMHS relative to a human subject, potentially resulting in different injuries. A method to compensate for this limitation is to test the PMHS inverted, returning the abdominal contents to locations more similar to where the organs would be situated ante-mortem. However, this is not possible for all test situations, e.g. sled tests. Only four of the tests included in this dataset tested inverted PMHS [7]. Therefore, the vast majority of the data used to generate the injury risk curves may represent an altered abdominal response and damage outcome relative to a live human.

V. CONCLUSION

This study generated injury risk curves predicting AIS2+ and AIS3+ injuries for nine different predictors. The best predictors for AIS2+ injuries were PBF and P. The best predictors for AIS3+ injuries V*C and P, where V*C had narrower confidence intervals. Vmax and rate of pressure were not significant predictors for any of the injury risk functions. Vmax was a particularly poor predictor for this dataset. Pressure was a significant predictor for both injury thresholds, indicating pressure-based predictors continue to show promise for abdominal injury predictions.

VI. ACKNOWLEDGEMENTS

Research reported in this report was supported by the Research Consortium for Crashworthiness in Automated Driving Systems (RCCADS). The content is solely the responsibility of the authors and does not necessarily represent the official views of RCCADS, or its members.

VII. REFERENCES

[1] Klinich, K.D., Flannagan, C.A., Nicholson, K., Schneider, L.W., Rupp, J.D. (2010) Factors Associated with Abdominal Injury in Frontal, Farside, and Nearside Crashes. *Stapp Car Crash Journal*, **54**: pp. 73–91.

[2] Dissanaike, S., Kaufman, R., Mack, C.D., Mock, C., Bulger, E. (2008) The effect of reclined seats on mortality in motor vehicle collisions. *Journal of Trauma and Acute Care Surgery*, **64**(3): pp. 614–619.

[3] McMurry, T.L., Poplin, G.S., Shaw, G., Panzer, M.B. (2018) Crash safety concerns for out-of-position occupant postures: A look toward safety in highly automated vehicles. *Traffic Injury Prevention*, **19**(6): pp. 582–587.

[4] Schaefer, L.C., Junge, M., Vörös, I., Koçaslan, K., Becker, U. (2021) Odds ratios for reclined seating positions in real-world crashes. *Accident Analysis & Prevention*, **161**(106357): pp. 1–11.

[5] Foster, C.D., Hardy, W.N., Yang, K.H., King, A.I., Hashimoto, S. (2006) High-Speed Seatbelt Pretensioner Loading of the Abdomen. *Stapp Car Crash Journal*, **50**: p. 27.

[6] Hardy, W.N., Schneider, L.W., Rouhana, S.W. (2001) Abdominal impact response to rigid-bar, seatbelt, and airbag loading. *Stapp Car Crash Journal*, **45**: pp. 1–32.

[7] Howes, M.K., Hardy, W.N., Agnew, A.M., Hallman, J.J. (2015) Evaluation of the Kinematic Responses and Potential Injury Mechanisms of the Jejunum during Seatbelt Loading. *Stapp Car Crash Journal*, **59**: pp. 225–267.
[8] Lamielle, S., Vezin, P., *et al*. (2008) 3D deformation and dynamics of the human cadaver abdomen under seatbelt loading. *Stapp Car Crash Journal*, **52**: pp. 267–294.
[9] Ramachandra, R., Kang, Y.-S., *et al*. (2016) Biomechanical Responses of PMHS Subjected to Abdominal Seatbelt Loading. *Stapp Car Crash Journal*, **60**: pp. 59–87.
[10] Ramachandra, R., Kang, Y.-S., *et al*. (2022) Biomechanical responses of small female PMHS subjected to abdominal loading. *Proceedings of The IRCOBI Conference,* 2022, Porto, Portugal.
[11] Rouhana, S.W., El-Jawahri, R.E., Laituri, T.R. (2010) Biomechanical considerations for abdominal loading by seat belt pretensioners. *Stapp Car Crash Journal*, **54**: pp. 381–406.
[12] Steffan, H., Hofinger, M., *et al.* (2002) Abdominal responses to dynamically lap belt loading. *Proceedings of the IRCOBI Conference*, 2002, Munich, Germany.
[13] Trosseille, X., Le-Coz, J.-Y., Potier, P., Lassau, J.-P. (2002) Abdominal response to high-speed seatbelt loading. *Stapp Car Crash Journal*, **46**: pp. 71–79.
[14] Untaroiu, C.D., Bose, D., *et al*. (2012) Effect of seat belt pretensioners on human abdomen and thorax: Biomechanical response and risk of injuries. *The Journal of Trauma and Acute Care Surgery*, **72**(5): pp. 1304–1315.
[15] Kremer, M.A., Gustafson, H.M., *et al*. (2011) Pressure-based abdominal injury criteria using isolated liver and full-body post-mortem human subject impact tests. *Stapp Car Crash Journal*, **55**: pp. 317–350.
[16] Sparks, J.L., Bolte, J.H., *et al*. (2007) Using pressure to predict liver injury risk from blunt impact. *Stapp Car Crash Journal*, **51**(10): pp. 401–432.
[17] Ramachandra, R., Stammen, J., *et al*. (2023) Abdominal biofidelity assessment of 5th percentile female ATD responses relative to recently developed belt and bar loading corridors. *Traffic Injury Prevention*, **24**(sup1): pp. S16–S22.
[18] Suntay, B., Stammen, J., Carlson, M., Ramachandra, R. (2021) Abdominal and thoracic injury risk functions for the large omni-directional child (LODC) ATD. *Proceedings of the IRCOBI Conference*, 2021, Online.
[19] Wang, Z., McInnis, J., Benfant, L., Feng, Z., Lee, E. (2017) THOR 5th percentile female ATD design. *Proceedings of 25th International Technical Conference on the Enhanced Safety of Vehicles*, 2017, Detroit, Michigan, USA.
[20] Johannsen, H., Trosseille, X., Lesire, P., Beillas, P. (2012) Estimating Q-Dummy Injury Criteria Using the CASPER Project Results and Scaling Adult Reference Values. *Proceedings of the IRCOBI Conference*, 2012, Dublin, Ireland.
[21] Beillas, P., Alonzo, F., *et al.* (2012) Abdominal Twin Pressure Sensors for the Assessment of Abdominal Injuries in Q Dummies: In-Dummy Evaluation and Performance in Accident Reconstructions. *Stapp Car Crash Journal*, **56**: pp. 387–410.
[22] Guettler, A.J., Bianco, S.T., *et al.* (2023) Frontal-Crash Occupant Protection in the Rear Seat: Submarining and Abdomen/Pelvis Response in Midsized Male Surrogates. *Stapp Car Crash Journal*, **67.**
[23] Albert, D.L., Beeman, S.M., Kemper, A.R. (2017) A method for measuring pressures in the liver and spleen of post-mortem human surrogates during full-scale frontal sled tests. *Biomedical Sciences Instrumentation*, **53**: pp. 88–93.
[24] AAAM (2015) *The Abbreviated Injury Scale - 2015 Revision.* Association for the Advancement of Automotive Medicine, Chicago, IL, USA.
[25] ISO (2014) ISO/TS 18506: Procedure to construct injury risk curves for the evaluation of road user protection in crash tests.

VIII. APPENDIX

TABLE AI
DATA FOR INJURY RISK ANALYSES

Study	Sex	Age	Stature (cm)	Mass (kg)	AIS	PBF (kN)	Cmax (%)	Vmax (m/s)	Vmax*Cmax	V*C	Fmax*Cmax	P (kPa)	P' (kPa/ms)	P*P' (kPa2/ms)
Hardy et al. 2001	F	77	168	53	0	6.1	33.0	3.40	1.06	1.10	1.77	-	-	-
Hardy et al. 2001	M	78	170	52	0	4.1	36.0	2.90	0.76	0.80	1.12	-	-	-
Hardy et al. 2001	M	88	156	72	0	4.5	37.0	5.60	2.07	1.20	1.67	-	-	-
Steffan et al. 2002	M	47	190	75	0	-	33.6	-	-	-	-	-	-	-
Steffan et al. 2002	M	49	182	85	0	6.0	35.5	-	-	-	2.13	-	-	-
Steffan et al. 2002	F	73	162	71	0	4.9	41.7	-	-	-	2.05	-	-	-
Steffan et al. 2002	F	42.5	166	60	0	7.4	31.4	-	-	-	2.32	-	-	-
Steffan et al. 2002	M	58	174	100	0	5.5	47.4	-	-	-	2.61	-	-	-
Steffan et al. 2002	M	59	180	95.5	3	10.6	35.3	-	-	-	3.74	-	-	-
Steffan et al. 2002	M	50	175	75	0	11.3	39.7	-	-	-	4.49	-	-	-
Steffan et al. 2002	F	87	171	70.1	3	-	56.5	-	-	-	-	-	-	-
Steffan et al. 2002	M	66	169	52	3	12.6	54.6	-	-	-	6.88	-	-	-
Steffan et al. 2002	M	54	172	79.3	0	10.9	56.9	-	-	-	6.20	-	-	-
Steffan et al. 2002	F	95	151	43.5	0	-	57.5	-	-	-	-	-	-	-
Steffan et al. 2002	M	69	183	72.2	0	9.2	55.2	-	-	-	5.08	-	-	-
Steffan et al. 2002	F	84	148	52.2	0	12.4	60.5	-	-	-	7.50	-	-	-
Trosseille et al. 2002	M	76	175	78	2	6.1	29.6	8.20	2.42	1.13	1.80	-	-	-
Trosseille et al. 2002	M	81	168	70	2	7.0	25.0	11.30	2.83	1.69	1.76	-	-	-
Trosseille et al. 2002	M	85	165	51	4	10.3	32.3	11.50	3.72	2.10	3.33	-	-	-
Trosseille et al. 2002	F	64	149	45	0	7.5	28.2	11.40	3.21	1.15	2.10	-	-	-
Trosseille et al. 2002	F	86	150	50	2	7.6	30.0	11.70	3.50	0.85	2.27	-	-	-
Foster et al. 2006	M	24	180	95.7	2	9.5	43.7	9.42	4.12	1.80	4.15	88.8	15.25	1354
Foster et al. 2006	M	58	188	111.2	0	10.0	35.4	6.89	2.44	1.11	3.55	102.8	13.59	1397
Foster et al. 2006	M	80	166.8	57.6	3	7.9	55.0	13.30	7.31	4.13	4.36	186.3	35.58	6628
Foster et al. 2006	M	83	173	81.6	3	9.6	50.3	8.51	4.28	2.03	4.85	120.3	20.13	2422
Foster et al. 2006	M	85	168.5	80.7	0	5.7	27.4	6.31	1.73	0.58	1.57	79.7	12.89	1027
Foster et al. 2006	M	45	173.5	74.8	0	5.0	35.8	6.13	2.20	1.10	1.78	93.9	11.06	1038

Foster et al. 2006	M	59	169	62.1	0	5.8	38.2	7.54	2.88	1.17	2.20	-	-	-
Foster et al. 2006	F	86	159.1	37.9	0	3.1	25.8	5.35	1.38	0.57	0.80	34.6	6.26	216
Foster et al. 2006	F	86	159.1	37.9	0	2.8	24.6	3.95	0.97	0.44	0.68	27.0	5.84	158
Untaroiu et al. 2012	F	71	157	77	2	6.5	24.4	5.08	1.24	0.37	1.59	-	-	-
Untaroiu et al. 2012	M	70	178	77	2	5.1	27.8	6.57	1.83	0.56	1.43	-	-	-
Untaroiu et al. 2012	M	64	191	57	0	4.8	21.0	4.47	0.94	0.48	1.00	-	-	-
Untaroiu et al. 2012	M	70	180	68	0	4.6	23.8	4.40	1.05	0.67	1.10	-	-	-
Howes et al. 2015	M	73	179	53	3	7.6	53.5	2.65	1.45	0.81	4.04	-	-	-
Howes et al. 2015	M	78	175	50	2	7.9	54.1	2.42	1.31	0.88	4.25	-	-	-
Howes et al. 2015	M	87	161	33	2	6.1	57.0	2.57	1.49	0.72	3.49	-	-	-
Howes et al. 2015	M	76	185	74	2	6.6	47.9	2.74	1.35	0.92	3.16	-	-	-
Howes et al. 2015	M	87	173	58	4	5.4	75.4	3.17	2.39	1.35	4.07	-	-	-
Howes et al. 2015	M	85	180	66	4	6.2	74.1	3.11	2.31	1.22	4.59	-	-	-
Ramachandra et al. 2016	M	59	170	86	3	4.2	46.0	3.40	1.56	1.12	1.93	67.0	2.40	161
Ramachandra et al. 2016	F	66	167	64	0	3.4	53.0	4.70	2.50	1.55	1.81	50.3	2.54	128
Ramachandra et al. 2016	M	66	180	70	0	3.6	45.0	3.90	1.74	1.24	1.63	65.4	2.84	186
Ramachandra et al. 2016	M	80	184	86	3	4.2	59.0	4.50	2.62	1.53	2.45	62.5	10.31	645
Ramachandra et al. 2016	F	75	166	50	0	3.4	72.0	3.50	2.50	1.64	2.46	21.7	1.87	41
Ramachandra et al. 2016	M	25	178	74	2	3.6	55.0	4.40	2.41	1.37	1.98	72.8	2.43	177
Ramachandra et al. 2016	M	48	174	67	3	4.8	52.0	5.20	2.69	1.88	2.47	38.0	8.25	314
Ramachandra et al. 2022	F	38	172	54	0	2.5	34.0	4.10	1.39	1.22	0.85	99.2	8.02	796
Ramachandra et al. 2022	M	73	175	61	0	2.7	30.0	3.70	1.10	0.94	0.81	50.4	3.58	180
Ramachandra et al. 2022	F	86	154.5	43	0	1.9	26.0	3.10	0.81	0.74	0.49	53.3	4.91	262
Ramachandra et al. 2022	F	83	175.5	55	4	4.3	45.0	3.30	1.48	0.83	1.94	104.5	5.80	606
Ramachandra et al. 2022	F	95	156	55	4	4.9	50.0	3.80	1.89	1.10	2.45	127.5	12.90	1645
Ramachandra et al. 2022	F	102	152.4	37	0	5.5	36.0	3.10	1.12	1.04	1.98	245.0*	31.50*	7718*
Guettler et al. 2023	M	79	178	63	4	10.8	-	-	-	-	-	99.9	4.70	469
Guettler et al. 2023	M	65	168	85	4	14.8	-	-	-	-	-	134.2	6.27	842
Guettler et al. 2023	M	83	175	81	5	13.6	-	-	-	-	-	118.7	6.59	782
Guettler et al. 2023	M	68	188	89	2	12.2	-	-	-	-	-	77.6	3.31	257
Guettler et al. 2023	M	59	173	68	3	9.8	-	-	-	-	-	126.3	4.52	570
Guettler et al. 2023	M	74	178	79	3	9.4	-	-	-	-	-	91.9	3.45	317
Guettler et al. 2023	M	63	180	81	2	17.1	-	-	-	-	-	120.2	9.89	1189
Guettler et al. 2023	M	51	168	64	4	13.9	-	-	-	-	-	149.4	8.64	1290

Guettler et al. 2023	M	51	175	89	4	17.1	-	-	-	-	-	330.4*	21.32*	7043*
Guettler et al. 2023	M	74	178	89	0	12.5	-	-	-	-	-	107.1	4.85	520
Guettler et al. 2023	M	74	170	64	3	10.4	-	-	-	-	-	127.2	5.98	760
Guettler et al. 2023	M	29	163	73	3	12.2	-	-	-	-	-	110.9	5.65	626

* indicates data that were excluded from the analysis

TABLE AII
SAMPLE SIZES FOR EACH PREDICTOR

	N	AIS2+		AIS3+	
		No Injury	Injury	No Injury	Injury
PBF	62	28	34	40	22
Cmax	53	29	24	39	14
Vmax	53	29	24	39	14
*Vmax*Cmax*	40	19	21	29	11
*V*C*	40	19	21	29	11
*Fmax*Cmax*	40	19	21	29	11
P	50	27	23	37	13
P'	31	12	19	16	15
*P*P'*	31	12	19	16	15

TABLE AIII
PEARSON CORRELATION COEFFICIENTS (UPPER TRIANGLE) AND P-VALUES (LOWER TRIANGLE) FROM LINEAR CORRELATION ANALYSIS OF PARAMETERS OF INTEREST
P-VALUES LESS THAN 0.05 ARE BOLDED

Predictors	PBF	Cmax	Vmax	Vmax*Cmax	V*C	Fmax*Cmax	P	P'	P*P'
PBF	-	0.1851	0.5815	0.5563	0.3566	0.8541	0.6584	0.1337	0.2014
Cmax	0.1982	-	-0.2871	0.2803	0.4073	0.6400	0.1349	0.1009	0.1917
Vmax	**<.0001**	0.0724	-	0.7951	0.5511	0.1941	0.6723	0.9122	0.8681
*Vmax*Cmax*	**0.0002**	0.0798	**<.0001**	-	0.8794	0.5714	0.6618	0.8456	0.8685
*V*C*	**0.0239**	**0.0091**	**0.0002**	**<.0001**	-	0.5114	0.5998	0.7365	0.8213
*Fmax*Cmax*	**<.0001**	**<.0001**	0.2300	**0.0001**	**0.0007**	-	0.6145	0.7159	0.6582
P	**<.0001**	0.5707	**0.0012**	**0.0015**	**0.0052**	**0.0039**	-	0.5604	0.6787
P'	0.4735	0.6720	**<.0001**	**<.0001**	**0.0002**	**0.0004**	**0.001**	-	0.9466
*P*P'*	0.2773	0.4182	**<.0001**	**<.0001**	**<.0001**	**0.0016**	**<.0001**	**<.0001**	-

TABLE AIV
INJURY RISK CURVE PARAMETERS FOR PREDICTING AIS2+ INJURIES

	Lognormal		Weibull		Loglogistic		Logistic	
	μ	σ	λ	κ	μ	σ	μ	σ
PBF	1.7854	0.8412	8.2738	1.2420	1.7783	0.5185	6.4783	3.9555
Cmax	3.8008	0.8049	58.0948	1.5149	3.8018	0.4911	46.6209	20.3835
Vmax	1.3628	3.5206	10.7751	0.3779	1.3641	2.2275	4.7012	7.6312
*Vmax*Cmax*	0.5765	0.7816	2.4101	1.3685	0.5699	0.4922	1.9241	1.0475
*V*C*	-0.0451	1.3074	1.4378	0.9889	-0.0382	0.8135	1.0547	0.7478
*Fmax*Cmax*	0.9682	1.1070	4.1868	0.8954	0.9522	0.6729	3.0867	3.3651
P	4.2091	0.5892	86.0678	2.0443	4.2153	0.3574	73.9283	25.4364
P'	1.0511	2.6869	7.2586	0.3915	1.0460	1.6769	1.5219	13.1461
*P*P'*	5.6727	1.7836	572.1132	0.5550	5.6566	1.0918	310.7348	785.9661

TABLE AV
INJURY RISK CURVE PARAMETERS FOR PREDICTING AIS3+ INJURIES

	Lognormal		Weibull		Loglogistic		Logistic	
	μ	σ	λ	κ	μ	σ	μ	σ
PBF	2.3103	0.9765	13.6262	1.3177	2.3115	0.5929	10.6455	4.7109
Cmax	4.0465	0.4268	65.4627	3.1383	4.0458	0.2525	57.8615	11.9647
Vmax	-	-	-	-	-	-	48.0282	43.7928
*Vmax*Cmax*	1.2408	0.8865	4.4484	1.5285	1.2512	0.5439	3.6002	1.3759
*V*C*	0.4950	0.6037	1.9237	2.3532	0.4962	0.3560	1.6560	0.4384
*Fmax*Cmax*	1.5264	0.8855	6.4448	1.3747	1.5252	0.5388	5.8457	2.9529
P	4.4526	0.6458	105.8916	2.2839	4.4710	0.3760	93.0262	26.7139
P'	1.9498	2.4300	16.0301	0.4627	1.9490	1.5395	8.8513	14.7407
*P*P'*	6.3456	1.8448	1138.1998	0.5925	6.3367	1.1586	813.4169	1040.4029

TABLE AVI
P-VALUES FOR GOODMAN KRUSKAL GAMMA AND CHI SQUARED (LOGISTIC) FOR AIS2+
P-VALUES LESS THAN 0.05 ARE BOLDED

	Lognormal	Weibull	Loglogistic	Logistic	Logistic
	γ p-value	γ p-value	γ p-value	γ p-value	χ^2 p-value
PBF	**0.0041**	**0.0032**	**0.0041**	**0.0079**	**0.0046**
Cmax	**0.0138**	**0.0148**	**0.0138**	**0.0350**	**0.0293**
Vmax	0.7840	0.9731	0.7840	0.6224	0.2580
*Vmax*Cmax*	0.1347	0.2255	0.1347	0.3394	**0.0278**
*V*C*	0.8556	0.8556	0.8556	0.6736	0.0890
*Fmax*Cmax*	**0.0333**	**0.0333**	0.0751	**0.0333**	0.0610
P	**0.0231**	**0.0231**	**0.0231**	0.0724	**0.0089**
P'	0.4229	0.4229	0.4229	-	0.3238
*P*P'*	**0.0231**	**0.0231**	**0.0231**	**0.0231**	0.1463

TABLE AVII
P-VALUES FOR GOODMAN KRUSKAL GAMMA AND CHI SQUARED (LOGISTIC) FOR AIS3+
P-VALUES LESS THAN 0.05 ARE BOLDED

	Lognormal γ p-value	Weibull γ p-value	Loglogistic γ p-value	Logistic γ p-value	Logistic χ^2 p-value
PBF	**0.0310**	0.0712	**0.0310**	0.2494	**0.0084**
Cmax	0.3103	0.1597	0.3103	0.1597	**0.0038**
Vmax	-	-	-	-	0.8478
*Vmax*Cmax*	0.1677	0.1677	0.1677	0.0321	0.0500
*V*C*	**0.0412**	**0.0412**	**0.0412**	**0.0412**	**0.0197**
*Fmax*Cmax*	0.6019	0.9732	0.6019	0.8375	**0.0242**
P	**0.0276**	**0.0076**	**0.0276**	**0.0365**	**0.0109**
P'	0.9202	0.9202	0.9202	0.8430	0.3053
*P*P'*	0.0921	0.3466	0.0921	0.9307	0.1866

TABLE AVIII
P-VALUES FOR POINT-BISERIAL CORRELATION COEFFICIENTS FOR AIS2+
P-VALUES LESS THAN 0.05 ARE BOLDED

	Lognormal	Weibull	Loglogistic	Logistic
PBF	**0.0008**	**0.0010**	**0.0008**	**0.0018**
Cmax	**0.0230**	**0.0217**	**0.0224**	**0.0208**
Vmax	0.5271	0.4884	0.5291	0.2757
*Vmax*Cmax*	**0.0091**	**0.0105**	**0.0095**	**0.0140**
*V*C*	0.1056	0.0892	0.1064	0.0654
*Fmax*Cmax*	**0.0062**	**0.0098**	**0.0060**	**0.0419**
P	**0.0024**	**0.0022**	**0.0025**	**0.0023**
P'	0.3252	0.3252	0.3265	0.3306
*P*P'*	**0.0310**	**0.0366**	**0.0305**	0.0839

TABLE AIX
P-VALUES FOR POINT-BISERIAL CORRELATION COEFFICIENTS FOR AIS3+
P-VALUES LESS THAN 0.05 ARE BOLDED

	Lognormal	Weibull	Loglogistic	Logistic
PBF	**0.0041**	**0.0040**	**0.0041**	**0.0045**
Cmax	**0.0008**	**0.0011**	**0.0009**	**0.0013**
Vmax	-	-	-	0.8351
*Vmax*Cmax*	**0.0237**	**0.0224**	**0.0243**	**0.0240**
*V*C*	**0.0031**	**0.0025**	**0.0030**	**0.0023**
*Fmax*Cmax*	**0.0063**	**0.0096**	**0.0070**	**0.0239**
P	**0.0048**	**0.0028**	**0.0044**	**0.0021**
P'	0.2700	0.2777	0.2725	0.3136
*P*P'*	**0.0444**	0.0517	**0.0455**	0.1085

TABLE AX

RELATIVE SIZE OF 95% CONFIDENCE INTERVALS AT 5%, 25%, AND 50% INJURY RISK FOR AIS2+ INJURIES

	Lognormal			Weibull			Loglogistic		
	5%	25%	50%	5%	25%	50%	5%	25%	50%
PBF	1.90	1.03	0.57	2.97	1.40	0.64	2.15	1.06	0.58
Cmax	2.24	1.01	0.58	3.02	1.18	0.54	2.53	1.04	0.58
Vmax	35.38	2269.50	3.02	37.63	919.62	2.59	40.22	3019.33	3.07
*Vmax*Cmax*	2.13	1.14	0.65	3.31	1.53	0.71	2.46	1.20	0.68
*V*C*	5.38	3.18	1.05	6.34	3.17	0.95	6.15	3.39	1.06
*Fmax*Cmax*	2.69	1.37	0.82	4.63	2.09	0.94	3.06	1.40	0.82
P	1.77	1.07	0.65	2.45	1.26	0.64	2.03	1.14	0.67
P'	19.77	151.08	3.76	28.14	374.74	4.03	21.99	167.17	3.76
*P*P'*	6.71	5.97	1.93	10.88	11.56	2.27	7.39	6.04	1.92

TABLE AXI

RELATIVE SIZE OF 95% CONFIDENCE INTERVALS AT 5%, 25%, AND 50% INJURY RISK FOR AIS3+ INJURIES

	Lognormal			Weibull			Loglogistic		
	5%	25%	50%	5%	25%	50%	5%	25%	50%
PBF	1.91	0.82	0.81	2.59	0.95	0.71	2.22	0.86	0.80
Cmax	0.70	0.36	0.44	0.96	0.39	0.38	0.83	0.37	0.43
Vmax	-	-	-	-	-	-	-	-	-
*Vmax*Cmax*	1.87	0.82	1.17	2.46	0.91	1.00	2.25	0.88	1.17
*V*C*	1.18	0.57	0.75	1.55	0.60	0.64	1.37	0.59	0.72
*Fmax*Cmax*	1.58	0.76	1.01	2.34	0.91	0.98	1.88	0.80	1.02
P	1.77	0.96	0.62	2.07	0.95	0.50	2.03	1.01	0.61
P'	13.37	16.80	2.20	19.17	29.69	2.24	15.40	19.06	2.25
*P*P'*	6.03	3.97	1.71	9.23	6.17	1.80	7.01	4.31	1.77

TABLE AXII

DAMAGE SUMMARY FOR EACH TEST

AIS2+, AIS3+, SOLID ORGAN INJURY, HOLLOW ORGAN INJURY, AND OTHER ABDOMINAL INJURY ARE BINARY, WHERE 0 REPRESENTS NO INJURY PRESENT AND 1 REPRESENTS THE PRESENCE OF THAT INJURY TYPE

Study	Sex	Age	AIS	AIS2+	AIS3+	Solid Organ Injury	Hollow Organ Injury	Other Abdominal Injury*
Hardy et al. 2001	F	77	0	0	0	0	0	0
Hardy et al. 2001	M	78	0	0	0	0	0	0
Hardy et al. 2001	M	88	0	0	0	0	0	0
Steffan et al. 2002	M	47	0	0	0	0	0	0
Steffan et al. 2002	M	49	0	0	0	0	0	0
Steffan et al. 2002	F	73	0	0	0	0	0	0
Steffan et al. 2002	F	42.5	0	0	0	0	0	0
Steffan et al. 2002	M	58	0	0	0	0	0	0
Steffan et al. 2002	M	59	3	1	1	0	1	0
Steffan et al. 2002	M	50	0	0	0	0	0	0
Steffan et al. 2002	F	87	3	1	1	0	1	1
Steffan et al. 2002	M	66	3	1	1	0	1	1
Steffan et al. 2002	M	54	0	0	0	0	0	0
Steffan et al. 2002	F	95	0	0	0	0	0	0
Steffan et al. 2002	M	69	0	0	0	0	0	0
Steffan et al. 2002	F	84	0	0	0	0	0	0

Trosseille et al. 2002	M	76	2	1	0	0	0	1
Trosseille et al. 2002	M	81	2	1	0	0	1	1
Trosseille et al. 2002	M	85	4	1	1	1	0	1
Trosseille et al. 2002	F	64	0	0	0	0	0	0
Trosseille et al. 2002	F	86	2	1	0	0	0	1
Foster et al. 2006	M	24	2	1	0	1	0	0
Foster et al. 2006	M	58	0	0	0	0	0	0
Foster et al. 2006	M	80	3	1	1	1	0	0
Foster et al. 2006	M	83	3	1	1	1	0	0
Foster et al. 2006	M	85	0	0	0	0	0	0
Foster et al. 2006	M	45	0	0	0	0	0	0
Foster et al. 2006	M	59	0	0	0	0	0	0
Foster et al. 2006	F	86	0	0	0	0	0	0
Foster et al. 2006	F	86	0	0	0	0	0	0
Untaroiu et al. 2012	F	71	2	1	0	1	0	0
Untaroiu et al. 2012	M	70	2	1	0	1	0	0
Untaroiu et al. 2012	M	64	0	0	0	0	0	0
Untaroiu et al. 2012	M	70	0	0	0	0	0	0
Howes et al. 2015	M	73	3	1	1	0	1	1
Howes et al. 2015	M	78	2	1	0	1	0	1
Howes et al. 2015	M	87	2	1	0	0	1	0
Howes et al. 2015	M	76	2	1	0	0	1	0
Howes et al. 2015	M	87	4	1	1	1	1	0
Howes et al. 2015	M	85	4	1	1	1	1	1
Ramachandra et al. 2016	M	59	3	1	1	1	0	0
Ramachandra et al. 2016	F	66	0	0	0	0	0	0
Ramachandra et al. 2016	M	66	0	0	0	0	0	0
Ramachandra et al. 2016	M	80	3	1	1	0	1	1
Ramachandra et al. 2016	F	75	0	0	0	0	0	0
Ramachandra et al. 2016	M	25	2	1	0	0	0	1
Ramachandra et al. 2016	M	48	3	1	1	0	1	0
Ramachandra et al. 2022	F	38	0	0	0	0	0	0
Ramachandra et al. 2022	M	73	0	0	0	0	0	0
Ramachandra et al. 2022	F	86	0	0	0	0	0	0
Ramachandra et al. 2022	F	83	4	1	1	1	1	0
Ramachandra et al. 2022	F	95	4	1	1	1	1	0
Ramachandra et al. 2022	F	102	0	0	0	0	0	0
Guettler et al. 2023	M	79	4	1	1	0	1	1
Guettler et al. 2023	M	65	4	1	1	1	1	1
Guettler et al. 2023	M	83	5	1	1	1	1	1
Guettler et al. 2023	M	68	2	1	0	1	0	1
Guettler et al. 2023	M	59	3	1	1	1	1	1
Guettler et al. 2023	M	74	3	1	1	0	1	1
Guettler et al. 2023	M	63	2	1	0	1	1	0
Guettler et al. 2023	M	51	4	1	1	1	1	1
Guettler et al. 2023	M	51	4	1	1	1	1	1
Guettler et al. 2023	M	74	0	0	0	0	0	0
Guettler et al. 2023	M	74	3	1	1	0	0	1
Guettler et al. 2023	M	29	3	1	1	0	0	1
Totals:	-	-	-	35	23	19	21	21

* Other abdominal injury includes damage to the mesentery, vessels, peritoneum, etc. Columns

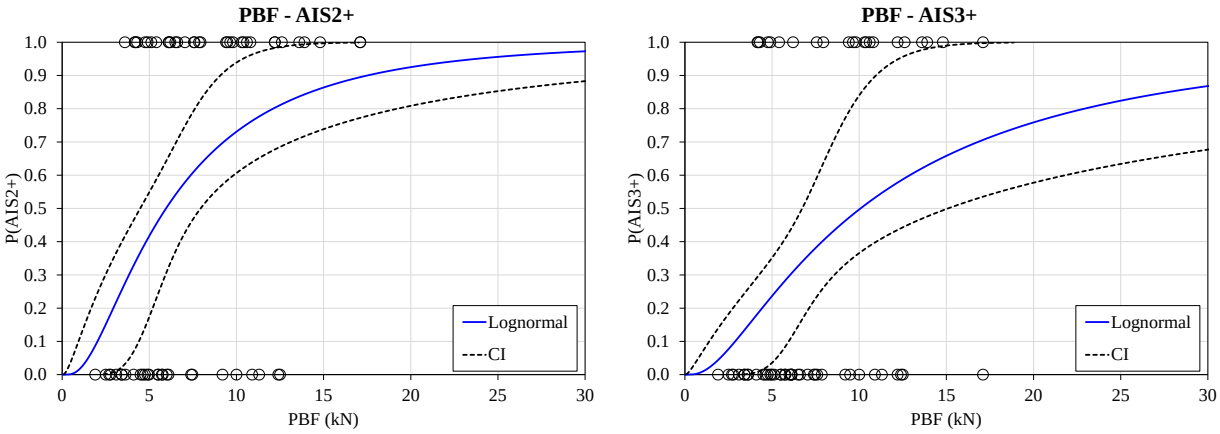

Fig. A1. Lognormal injury risk functions and 95% confidence intervals using Peak Belt Force for AIS2+ (left) and AIS3+ (right) injuries.

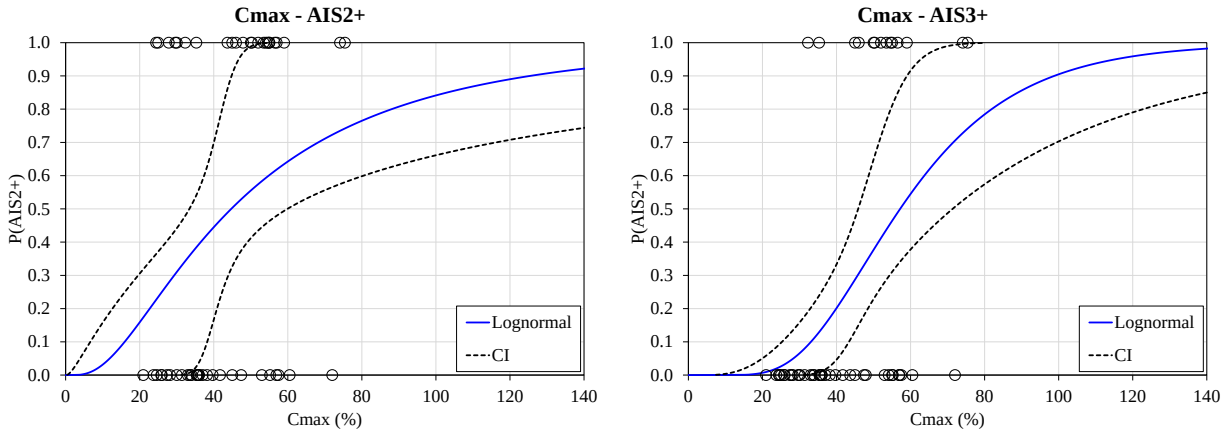

Fig. A2. Lognormal injury risk functions and 95% confidence intervals using Cmax for AIS2+ (left) and AIS3+ (right) injuries.

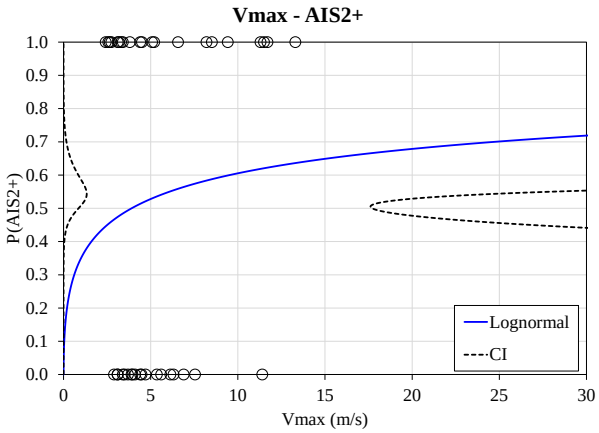

Fig. A3. Lognormal injury risk function and 95% confidence interval using Vmax for AIS2+ injuries.

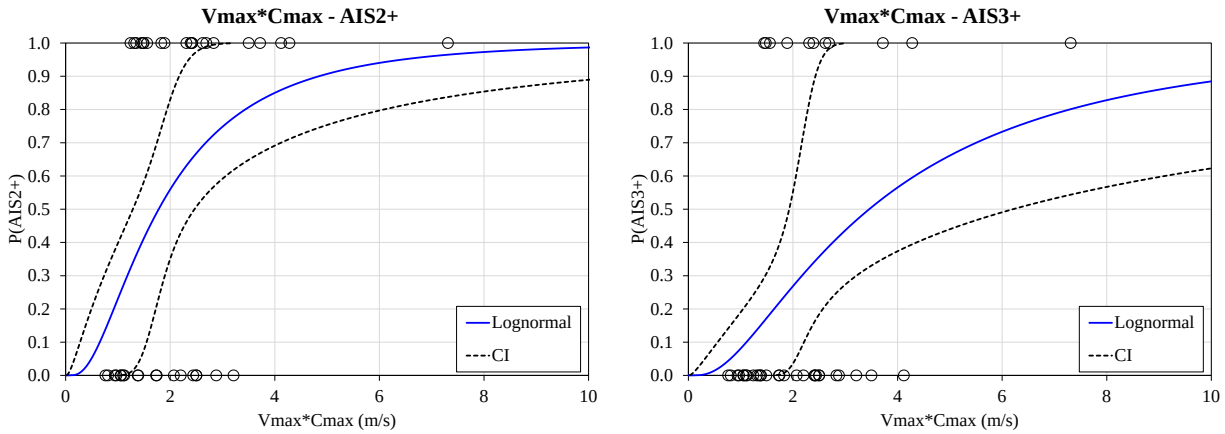

Fig. A4. Lognormal injury risk functions and 95% confidence intervals using Vmax*Cmax for AIS2+ (left) and AIS3+ (right) injuries.

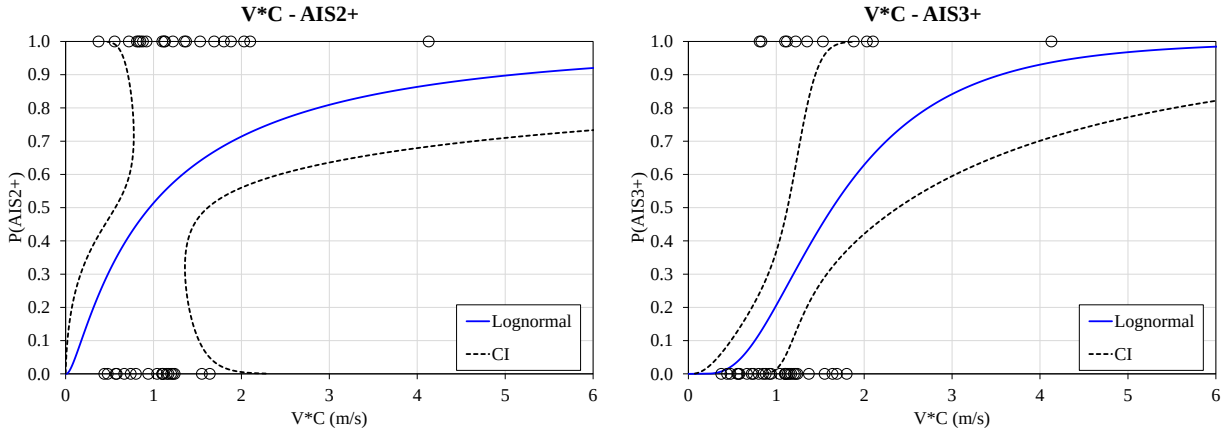

Fig. A5. Lognormal injury risk functions and 95% confidence intervals using V*C for AIS2+ (left) and AIS3+ (right) injuries.

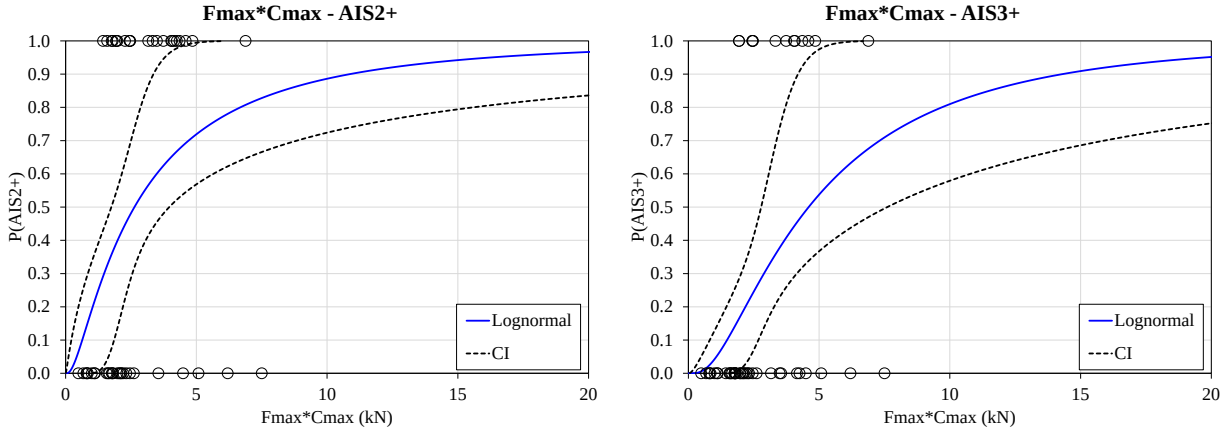

Fig. A6. Lognormal injury risk functions and 95% confidence intervals using Fmax*Cmax for AIS2+ (left) and AIS3+ (right) injuries.

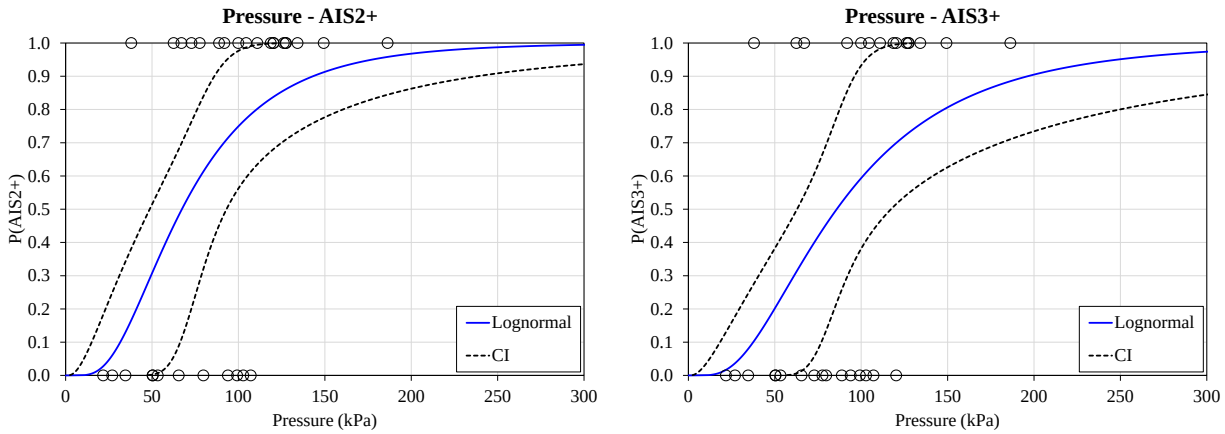

Fig. A7. Lognormal injury risk functions and 95% confidence intervals using Pressure for AIS2+ (left) and AIS3+ (right) injuries.

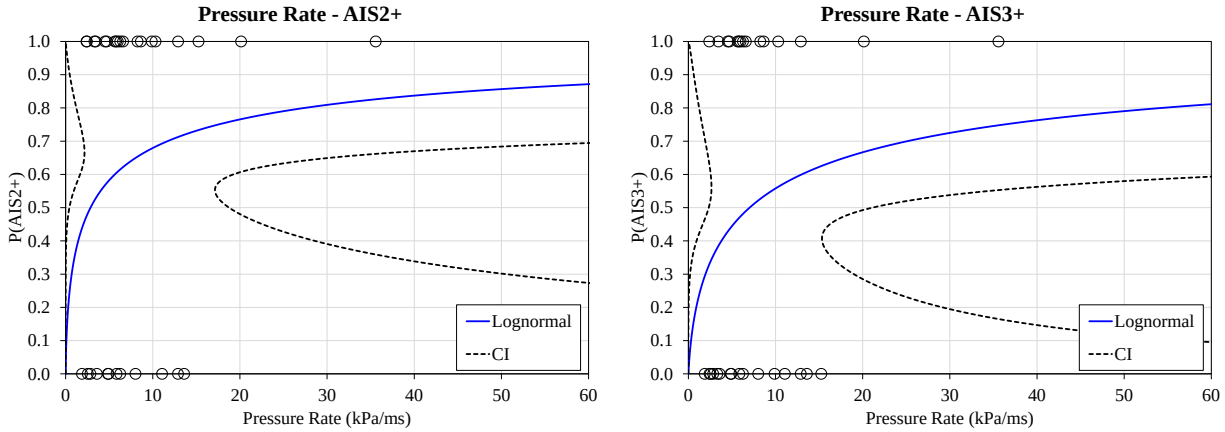

Fig. A8. Lognormal injury risk functions and 95% confidence intervals using Pressure Rate for AIS2+ (left) and AIS3+ (right) injuries.

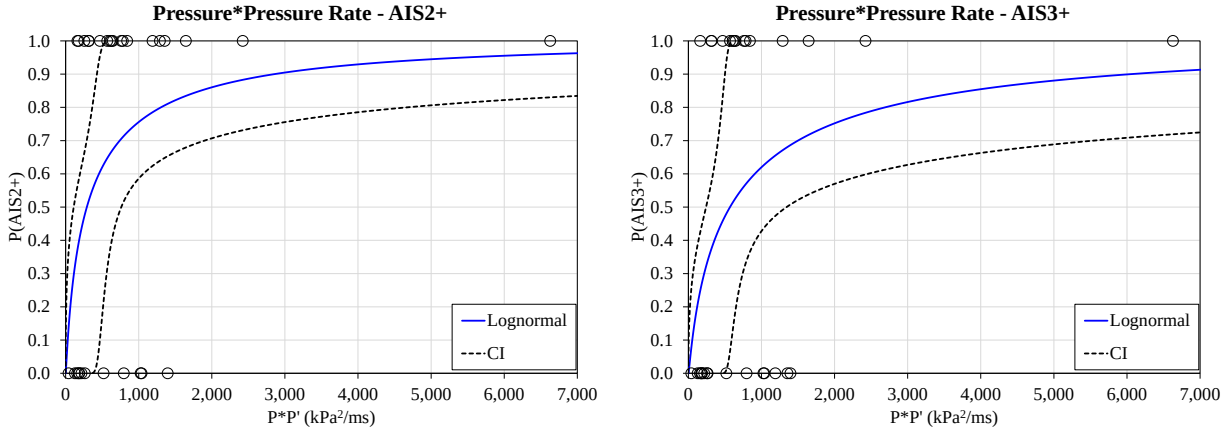

Fig. A9. Lognormal injury risk functions and 95% confidence intervals using Pressure Rate for AIS2+ (left) and AIS3+ (right) injuries.

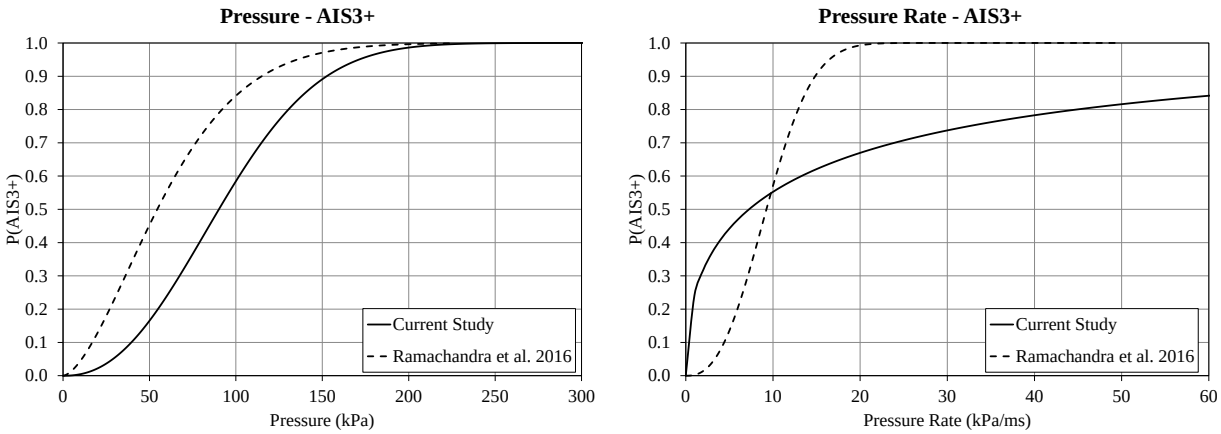

Fig. A10. Comparison of Weibull AIS3+ injury risk curves from the current study and Ramachandra et al. 2016 studies for Pressure (left) and Pressure Rate (right).

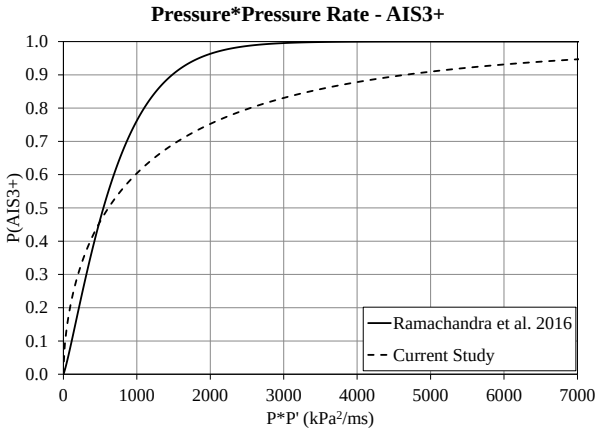

Fig. A11. Comparison of Weibull AIS3+ injury risk curves from the current study and Ramachandra et al. 2016 studies for Pressure*Pressure Rate.